

Long-Range Transformers for Dynamic Spatiotemporal Forecasting

Jake Grigsby, Zhe Wang, Yanjun Qi

Univeristy of Virginia
{jcg6dn, zw6sg, yanjun}@virginia.edu

Abstract

Multivariate Time Series Forecasting (TSF) focuses on the prediction of future values based on historical context. In these problems, dependent variables provide additional information or early warning signs of changes in future behavior. State-of-the-art forecasting models rely on neural attention between timesteps. This allows for *temporal* learning but fails to consider distinct *spatial* relationships between variables. This paper addresses the problem by translating multivariate TSF into a novel “spatiotemporal sequence” formulation where each input token represents the value of a single variable at a given timestep. Long-Range Transformers can then learn interactions between space, time, and value information jointly along this extended sequence. Our method, which we call `Spacetimeformer`, scales to high dimensional forecasting problems dominated by Graph Neural Networks that rely on predefined variable graphs. We achieve competitive results on benchmarks from traffic forecasting to electricity demand and weather prediction while learning spatial and temporal relationships purely from data.

1 Introduction

Multivariate forecasting attempts to predict future outcomes based on historical context and has direct applications to many domains, including science, policy, and business. Jointly modeling a set of variables allows us to interpret dependency relationships that provide additional context or early warning signs for changes in future behavior. Time Series Forecasting (TSF) models typically deal with a small number of variables with long-term *temporal* dependencies that require historical recall and distant forecasting. This is commonly handled by encoder-decoder sequence-to-sequence (Seq2Seq) architectures (Sec 2.1). The relationships between input variables are usually unknown, sparse, or time-dependent. Examples include many health and finance applications. In these cases, we are forced to discover variable relationships from data. Current state-of-the-art TSF models substitute classic Seq2Seq architectures for neural-attention-based mechanisms (Zhou et al. 2021). However, these models represent the value of multiple vari-

ables per timestep as a single input token¹. This only allows them to learn “temporal attention” amongst timesteps, and can ignore the distinct *spatial*² relationships that exist between variables.

In this paper, we propose to flatten multivariate inputs into long sequences where each input token isolates the value of a single variable at a given timestep. The resulting input allows Long-Range Transformer architectures to learn self-attention networks across both space and time jointly. This creates a “spatiotemporal attention” mechanism. Figure 1 illustrates the distinction between temporal and spatiotemporal attention. Our method can interpret long context windows and forecast many timesteps into the future while also discovering the spatial relationships between hundreds of variables. The spatial scalability of our model suggests applications to the kinds of forecasting problems currently dominated by Graph Neural Network (GNN) methods. GNNs rely on predefined graphs representing the relationships between input variables. We empirically show that spatiotemporal sequence learning with Transformers can recover the relationships necessary to achieve competitive performance on these tasks while learning spatial and temporal connections purely from data. We evaluate the technique in various domains spanning the spatiotemporal spectrum from traffic forecasting to electricity production and long-term weather prediction.

2 Background and Related Work

2.1 Deep Learning in Time Series Forecasting

TSF in practice is often focused on business/finance applications and utilizes relatively simple but reliable statistical methods (Box et al. 2015) (Taylor and Letham 2018). Analogous to the trend in areas like Vision and Natural Language Processing (NLP), hand-crafted approaches have begun to be replaced by Deep Learning techniques (Smyl 2020). This is particularly true in multivariate forecasting,

¹An *input token* is one element of a Transformer’s input sequence. Multihead Self-Attention (Sec 2.2) learns representations by sharing information between tokens.

²In most real-world forecasting tasks, variables spatially close to one another exhibit similar patterns. We use the word “spatial” to refer to such relationships between multiple variables generally.

where the relationships between multiple time series challenge traditional models’ ability to scale (Lim and Zohren 2021) (Benidis et al. 2020). Deep Learning approaches to TSF are generally based on a Seq2Seq framework in which a *context window* of the recent past is mapped to a *target window* of predictions for the future. More formally: given a sequence of time inputs $\{x_{T-c}, \dots, x_T\}$ and variable(s) $\{y_{T-c}, \dots, y_T\}$ up to time T , we output another sequence of variable values $\{\hat{y}_{T+1}, \dots, \hat{y}_{T+t}\}$ corresponding to our predictions at future timesteps $\{x_{T+1}, \dots, x_{T+t}\}$.

The most common class of deep TSF models are based on a combination of Recurrent Neural Networks (RNNs) and one-dimensional convolutions (Conv1Ds) (Borovykh, Bohte, and Oosterlee 2017) (Smyl 2020) (Salinas, Flunkert, and Gasthaus 2019) (Lai et al. 2018). More related to the proposed method is a recent line of work on attention mechanisms that aim to overcome RNNs’ autoregressive training and difficulty in interpreting long-term patterns (Iwata and Kumagai 2020) (Li et al. 2019) (Zerveas et al. 2020) (Wu et al. 2020a) (Oreshkin et al. 2020). Notable among these is the `Informer` (Zhou et al. 2021) - a general encoder-decoder Transformer architecture for TSF. `Informer` encodes time series inputs with learned temporal embeddings and appends a *start token*³ to the decoder sequence of zeros that need prediction.

2.2 Long-Range Transformers

The Transformer (Vaswani et al. 2017) is a Deep Learning architecture for sequence-to-sequence prediction that is widely used in NLP (Devlin et al. 2019). Transformers are centered around the multi-head self-attention (MSA) mechanism. A sequence (x) consisting of L input tokens generates d -dimensional query, key, and value vectors with learned feed-forward layers denoted \mathbf{W}^Q , \mathbf{W}^K , and \mathbf{W}^V , respectively. The scaled dot-product of tokens’ query and key vectors determines the attention given to values along the input sequence according to Eq 1.

$$\text{MSA}(x) = \text{softmax} \left(\frac{\mathbf{W}^Q(x)\mathbf{W}^K(x)}{\sqrt{d}} \right) \mathbf{W}^V(x) \quad (1)$$

MSA learns weighted relationships between its inputs in order to pass information between tokens. This idea has appealing similarity to passing messages across a weighted adjacency matrix (a graph) (Joshi 2020) (Liu et al. 2019). Because MSA matches each query to the keys of the entire sequence, its runtime and memory use grows quadratically with the length of its input. This becomes a significant obstacle in long-input domains where self-attention might otherwise be a promising solution, including document classification (Pappagari et al. 2019), summarization (Manakul and Gales 2021), and protein sequence analysis (Lanchantin et al. 2021). As a result, the research community has raced to develop and evaluate MSA-variants for longer sequences (Tay et al. 2020). Many of these methods introduce heuristics to sparsify the attention matrix. For example, we can at-

³The start token is probably better described as a “start token sequence” because unlike special-purpose start tokens in NLP it is a sequence of the final tokens of the context window.

tend primarily to adjacent input tokens (Li et al. 2019), select global tokens (Guo et al. 2019), increasingly distant tokens (Ye et al. 2019) (Child et al. 2019) or a combination thereof (Zaheer et al. 2020) (Zhang et al. 2021). While these methods are effective, their inductive biases about the structure of the trained attention matrix are not always compatible with tasks outside of NLP.

Another approach looks to approximate MSA in sub-quadratic time while retaining its flexibility (Wang et al. 2020) (Zhou et al. 2021) (Xiong et al. 2021) (Zhu et al. 2021). Particularly relevant to this work is the `Performer` (Choromanski et al. 2021). `Performer` approximates MSA in linear space and time with a kernel of random orthogonal features and enables the long-sequence approach that is central to our work.

2.3 Spatiotemporal Forecasting

Multivariate TSF involves two axes of complexity: the forecast sequence’s duration, L , and the number of variables N considered at each timestep. As N grows, it becomes increasingly important to model the spatial relationships between each variable explicitly. Recent TSF methods structure their input as (x_t, y_t) concatenated vectors of multiple variable values per timestep. Attention-based models need to connect the variable values at a given timestep to entire timesteps in the past. However, the variables we are modeling may have different periodicities and relations to one another.

To better explain this, we introduce a TSF problem later used in our experiments. Suppose we are forecasting the air temperature at weather stations in the United States. Several stations are located relatively close to each other in central Texas. The rest are also clustered together but centered hundreds of miles away outside New York City. The two groups experience different weather patterns as a result of their geographic separation. In order to predict future weather patterns in Texas, we may need to attend to the values of nearby stations when the current weather cycle began. However, this may have occurred before the information that is relevant to the stations in New York. When faced with this problem, a temporal attention model would be forced to “average” these requirements and attend to timesteps somewhere in the middle - a compromise that provides little relevant information to either situation. The NY-TX weather problem is unrealistic in the sense that it is unlikely that a real-world system would attempt to jointly model such unrelated sequences. However, this problem can appear more subtly in domains where the relationships between the series are unknown or difficult to predict.

There have been a number of approaches that confront this problem in the context of RNN-based attention (Shih, Sun, and Lee 2019) (Gangopadhyay et al. 2021) (Qin et al. 2017). These models alternate between separate spatial and temporal layers. There are several works extending MSA to similar ‘spatial, then temporal’ architectures (Xu et al. 2021) (Cai et al. 2020) (Park et al. 2020) (Plizzari, Cannici, and Matteucci 2021), but they rely on the predefined variable graphs common in the GNN literature (see Sec 3.3). Further discussion is moved to Appendix A.

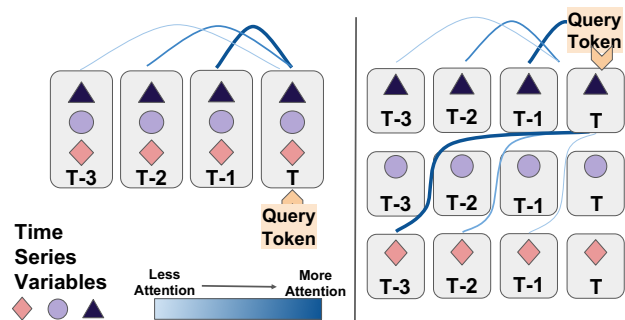


Figure 1: **Temporal learning (left) versus Spatiotemporal learning (right)**: Splitting the variables into separate tokens creates a spatiotemporal graph where we can attend to different timesteps for each variable.

3 Method

3.1 Spatiotemporal Forecasting with Transformers

The temporal attention compromise discussed in Sec 2.3 can be blamed on the fact that we are representing multiple variables per token. It is important to note that this dilemma is unique to applications of Transformers outside of NLP. In the NLP setting, every token of the input sequence represents one individual idea (e.g., a single word). However, multivariate TSF inherently models multiple distinct sequences per timestep (Shih, Sun, and Lee 2019). The solution, then, is to recover the “one-idea-per-token” format of NLP. We can do this by separating (x_t, y_t) inputs into a sub-sequence of $\{(x_t, y_t^1), \dots, (x_t, y_t^N)\}$ tokens, where N is the number of variables we are modeling. The resulting sequence is N times longer but represents each node of the spatiotemporal graph as an individual token. Assuming our attention mechanism can scale with the additional length, it can now learn unique relationships for every variable. The distinction is depicted in Figure 1.

After flattening the input variables, we need to allow Transformers to correctly interpret the variable each token originates from as well as its time and scalar value. Transformers are permutation invariant, meaning they cannot interpret the order of input tokens by default. This is fixed by adding a *position embedding* to the tokens - usually with a fixed sinusoidal pattern (Vaswani et al. 2017). In our flattened representation, N tokens should have the same position. This could be solved with a modified positional embedding that accounts for the flattened sequence. However, a fixed positional embedding only preserves relative order. In the NLP context, relative position is all that matters, but in a time series problem, the input sequence takes place in a specific window of time that may be relevant to long-term seasonal patterns. For example, it is important to know the relative order of three weeks of temperature observations, but it is also important to know that those three weeks take place in late spring when temperatures are typically rising. We achieve this by learning positional embeddings based on a *Time2Vec* layer (Kazemi et al. 2019). *Time2Vec* passes a representation of absolute time (e.g., the calendar datetime) through sinusoidal patterns of learned offsets and wavelengths. This helps represent periodic relationships that

are relevant to accurate predictions. We also append a relative order index to the time input values⁴. The concatenated timeseries value and time embedding are then projected to the input dimension of the Transformer model with a feed-forward layer. We refer to the resulting output as the “Value&Time Embedding.”

Now that the model can distinguish between timesteps, it also has to tell the difference between the variables at each of those timesteps. We add a “Variable Embedding” to each token. The variable embedding indicates the time series from which each token originates. This is implemented as a standard embedding layer that maps the integer index of each series to a higher-dimensional representation as is common for word embeddings in NLP.

A final consideration is the representation of missing timeseries values that the model is tasked to predict. The encoder observes the context sequence in which all values are present. However, the decoder deals with missing values that need prediction in addition to the start token of the last few timesteps of the context sequence (as in the *Informer* (Zhou et al. 2021) model). We pass missing values as a zero vector and resolve ambiguity between true context/start-token values of zero and missing tokens with a binary “Given embedding”⁵. The Value&Time, Space, and Given embeddings sum to create the encoded sequence. The entire pipeline is represented visually in Figure 2.

3.2 Long-Range Transformers for Real-World Spatiotemporal Forecasting

After the spatiotemporal embedding, the sequence is ready to be fed through a standard Transformer encoder-decoder. Our method does not assume access to predefined variable relationships or even that those relationships remain fixed over time; the embedding represents the spatiotemporal forecasting problem in a raw format that puts full faith in the learning power of the Transformer architecture. This may raise questions as to why this approach has not been tried before; the answer rests heavily on scale and timing. The embedding in Sec 3.1 converts a sequence-to-sequence problem of length L into a new one of length LN . Vanilla MSA layers have a maximum sequence length of less than 1,000 - and on hardware aside from the highest-end GPUs/TPUs we are limited to something closer to ~ 500 . The spatiotemporal sequence lengths considered in our experimental results exceed 23,000. Clearly, additional optimization is needed to make these problems feasible.

Scaling with Fast-Attention. However, we are fortunate that there is a rapidly-developing field of research in long-sequence transformers (Sec 2.2). We modify open-source implementations of fast-attention mechanisms in an effort

⁴This is helpful when the data are taken at close intervals such that most entries of the resulting *Time2Vec* output vectors are identical. In the extreme case, it serves as a fail-safe for datasets that do not provide distinct timestamps for each datapoint, e.g., when all observations occur on the same day but the hour and minute values are not recorded.

⁵The Given embedding is not used in *Informer* and is not often relevant in practice. It resolves an edge case for datasets that naturally contain zero values.

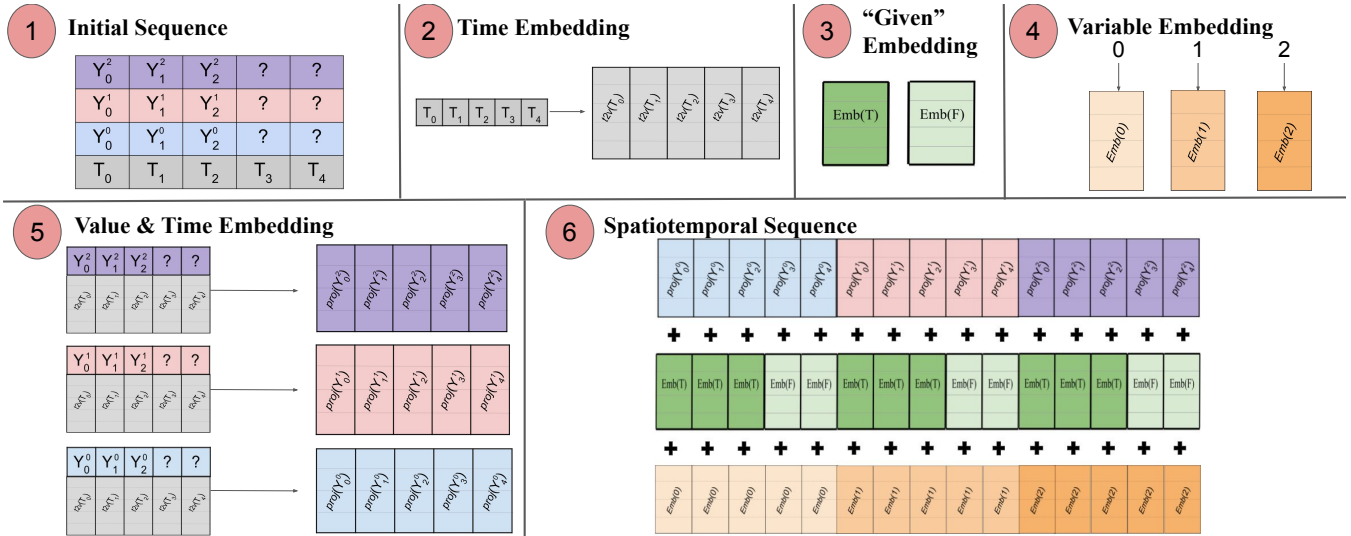


Figure 2: **Input Encoding Pipeline:** (1) The standard multivariate input format with time information included. Decoder inputs have missing (“?”) values set to zero where predictions will be made. (2) The time sequence is passed through a Time2Vec layer to generate a frequency embedding that represents periodic input patterns. (3) A binary embedding indicates whether this value is given as context or needs to be predicted. (4) The integer index of each time series is mapped to a “spatial” representation with a lookup-table embedding. (5) The Time2Vec embedding and variable values of each time series are projected with a feed-forward layer. (6) Value&Time, Variable, and Given embeddings are summed and laid out s.t. MSA attends to relationships across both time and variable space at the cost of a longer input sequence.

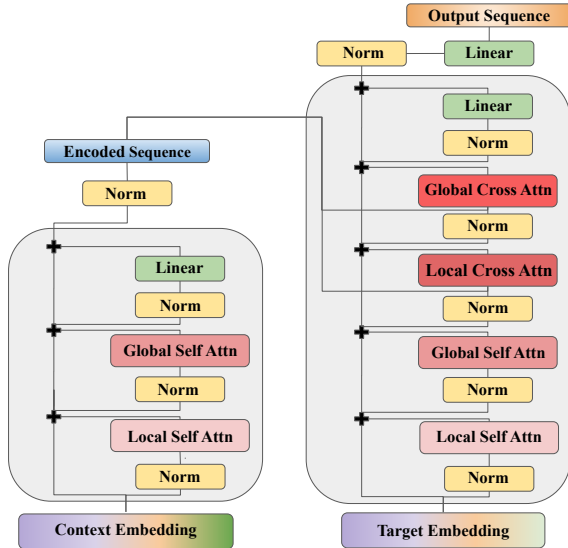


Figure 3: The Spacetimeformer architecture for joint spatiotemporal sequence learning.

to scale our model. Informer (Zhou et al. 2021) proposes ProbSparse attention. While this method is faster and more scalable than vanilla MSA, we are only able to reach sequences between 1k-2k tokens, mostly because it is only applicable to self-attention modules. Instead, we opt for the Performer FAVOR+ attention (Choromanski et al. 2021) - a linear approximation of softmax⁶ attention using a ran-

⁶In practice we find that the generalized ReLU kernel variant is slightly more memory efficient and use that as our default attention mechanism.

dom kernel method. The experiments in this paper are performed on four 8 – 12GB GPUs - significantly less memory than the maximum currently available (e.g., larger clusters of V100s, TPUs). This constraint is likely to be less relevant as hardware development continues to shift towards intensive Deep Learning. However, we find that a multi-GPU Performer setup is enough to tackle all but the longest spatiotemporal sequences.

Scaling with Initial and Intermediate Convs. In the longest-sequence problems, we can also look for ways to learn shorter representations of the input to save memory. This is only applicable to the context window encoder, but in practice the context window is typically the bottleneck. We can learn to summarize the sequence with strided one-dimensional convolutions; we use the proper stride and padding to cut sequence length in half per Conv1D layer. “Initial” convolutions are applied to the Value&Time embedding while the variable embedding tokens are repeated for half their usual length. “Intermediate” convolutions occur between MSA layers. Intermediate convolutions are a key component of the Informer (Zhou et al. 2021) architecture. However, our embedding creates an undesirable emphasis on the order of the flattened variable tokens. We address this by passing each variable’s full sequence through the convolution independently (halving their length) and then recombining them into the longer spatiotemporal sequence. We prefer to learn the full-size spatiotemporal graph when it fits in memory. Therefore none of the reported results use intermediate convolutions; the longest dataset (AL Solar) model uses one initial convolution.

Local and Global Attention. We empirically find that learning an attention layer over a longer global sequence

eliminates a helpful local bias that hurts performance in problems with large N . We address this by adding additional “local” attention modules to each encoder and decoder layer. Each variable sequence attends to itself first before attending to global tokens. Note that this does mean we are simplifying the global attention layer by separating temporal and spatial attention, as is common in the methods discussed above in addition to Video Transformers (Arnab et al. 2021) and other long-range NLP architectures (Zhu et al. 2021) (Zhang et al. 2021). Rather, every token attends to every token in its own sequence and then to every token in the entire spatiotemporal global sequence. We use a Pre-Norm architecture (Xiong et al. 2020) and BatchNorm normalization rather than the standard LayerNorm and other alternatives in the literature. Additional implementation details are discussed in Appendix C. A one-layer encoder-decoder architecture is depicted in Figure 3.

Output and Loss Functions. The final feed-forward layer of the decoder generates a two-dimensional vector that parameterizes the mean and standard deviation of a Normal distribution. This sequence of distributions is folded back into the original input format of (x_t, \hat{y}_t) , and the timesteps corresponding to predictions on the start tokens are discarded. We can then optimize a variety of forecasting loss functions, depending on the particular problem and the baselines we are comparing against. Explanations of common loss functions can also be found in Appendix C.

Because of all this additional engineering, we avoid direct comparisons to Informer although it is a key inspiration and closely related work. Instead, our most direct baseline is a version of our model that follows a “temporal-only” embedding scheme similar to Informer’s. The sequence is never flattened into distinct spatial tokens; the Value&Time embedding input includes all the time series values concatenated together as normal, and there is no spatial embedding. There is no concept of “local vs. global” in this setup, so we skip the local attention modules. We typically compensate for parameter count differences with additional encoder/decoder layers. We nickname our model the Spacetimeformer for clarity in experimental results.

3.3 Connecting to Spatial Forecasting and GNNs

As N approaches and then exceeds L , e.g., in traffic forecasting, we begin to enter the territory of Graph Neural Networks (Wu et al. 2021a). In this context, GNNs are multivariate forecasting models where the relationship between the time series can be provided in advance (e.g., a map of connected roads) (Liu et al. 2019) (Li et al. 2018). A typical forecasting GNN involves iterative applications of graph message passing between nodes (e.g., Graph Convolutional Network layers (Bruna et al. 2014)) followed by an RNN/Conv1D for temporal learning amongst the timesteps of each node individually. For a representative example and thorough explanation see DCRNN (Li et al. 2018).

This paper approaches multivariate prediction with Transformers from a TSF perspective where spatial relationships should be explicitly modeled, but their relationships are unknown and must be learned during training. We propose a novel input embedding and architecture for Transform-

	Variables (N)	Length (L)	Size (Timesteps)
NY-TX Weather	6	800	569,443
Toy Dataset	20	160	2,000
AL Solar	137	192	52,560
Metr-LA Traffic	207	24	34,272
Pems-Bay Traffic	325	24	52,116

Table 1: **Dataset Summary.**

ers that jointly learn spatial and temporal attention along an extended spatiotemporal sequence. In this way, we blur the distinction between TSF and GNN models. MTGNN (Wu et al. 2020b) is a related work in this hybrid category that learns an adjacency matrix from data before applying GNN-style spatial/temporal convolutions. However, it still separates spatial and temporal learning and is not as capable as a temporal forecaster because its one-shot convolutional prediction module does not scale with L like a TSF method. Our method retains the temporal forecasting ability of a TSF model while recovering the spatial relationships of a GNN model and avoiding the assumption of a predefined graph.

4 Experiments

We evaluate our method in five datasets, including traffic forecasting, weather prediction, solar energy production, and a simple toy example. Descriptions of each task can be found in Appendix B, and a summary of key information is provided in Table 1. We compare against representative methods from the TSF and GNN literature in addition to ablations of our model. These include the previously mentioned MTGNN model and Temporal ablation, as well as a basic autoregressive linear model (Linear AR), a standard encoder-decoder LSTM without attention, and a CNN/Conv1D-based LSTMNet (Lai et al. 2018). See Appendix C.2 for details. Hyperparameter information for Spacetimeformer models can be found in Appendix C.1. All results average at least three random seeds, with additional runs collected when variance is non-negligible. All models use the same training loop, dataset code, and evaluation process to ensure a fair comparison. We also add Time2Vec information to baseline inputs when applicable because it has been shown to improve the performance of a variety of sequence models (Kazemi et al. 2019).

Toy Dataset. We begin with a toy dataset inspired by (Shih, Sun, and Lee 2019) consisting of a multivariate sine-wave sequence with strong inter-variable dependence. More details can be found in Appendix B. Several ablations of our method are considered. Temporal modifies the spatiotemporal embedding as discussed at the end of Sec 3.2. ST Local skips the global attention layers but includes spatial information in the embedding. The “Deeper” variants attempt to compensate for the additional parameters of the local+global attention architecture of our full method. All models use a small Transformer model and optimize for MSE. The final quarter of the time series is held out as a test set; a similar test split is used in all experiments (Cerqueira, Torgo, and Mozetič 2020). The results are shown

	Temporal	Temporal (Deeper)	Temporal (Deeper & Full Attn)	ST Local	ST Local (Deeper)	Spacetimeformer
MSE	0.006	0.010	0.005	0.021	0.014	<u>0.003</u>
MAE	0.056	0.070	0.056	0.104	0.090	<u>0.042</u>
RRSE	0.093	0.129	0.094	0.180	0.153	<u>0.070</u>

Table 2: **Toy Dataset Results.** We indicate the loss function metric (here, MSE) with italics in subsequent tables.

in Table 2. The `Temporal` embedding is forced to compromise its attention over timesteps in a way that reduces predictive power over variables with such distinct frequencies. Standard (“Full”) attention fits in memory with the `Temporal` embedding but is well approximated by `Performer`. Our method learns an uncompromising spatiotemporal relationship among all tokens to generate the most accurate predictions by all three metrics.

NY-TX Weather. We evaluate each model on a custom dataset of temperature values collected from the ASOS Weather Network. As described in our Sec 2.3 example, we use three stations in central Texas and three in eastern New York. Temperature values are taken at one-hour intervals, and we investigate the impact of sequence length by predicting 40, 80, and 160 hour target sequences. The results are shown in Table 3. Our spatiotemporal embedding scheme provides the most accurate forecasts, and its improvement over the `Temporal` method appears to increase over longer sequences where the temporal attention compromise may be more relevant. `LSTM` is the most competitive baseline. This is not surprising given that this problem lies towards the TSF end of the spatiotemporal spectrum, where `LSTMs` are a common default. The success of `MTGNN` is more surprising because we are using it at sequence lengths far longer than considered in the original paper (Wu et al. 2020b). However, its convolution-only output mechanism begins to struggle at the 80 and 160 hour lengths.

We use the NY-TX weather dataset to experiment with a Negative Log Likelihood (NLL) loss that maximizes the probability of the target sequence and makes use of our output distributions’ uncertainty estimates. The model learns an intuitive prediction strategy that generally increases uncertainty along the target sequence. It also adds uncertainty to inflection points where temperatures are reaching daily lows or highs. An example prediction plot for one of the stations is shown in Appendix C.1 Figure 6.

	Linear AR	LSTM	MTGNN	Temporal	Spacetimeformer
40 hours					
MSE	18.84	14.29	13.32	13.29	<u>12.49</u>
MAE	3.24	2.84	2.67	2.67	<u>2.57</u>
RRSE	0.40	0.355	0.34	0.34	<u>0.33</u>
80 hours					
MSE	23.99	18.75	19.27	19.99	<u>17.9</u>
MAE	3.72	3.29	3.31	3.37	<u>3.19</u>
RRSE	0.45	<u>0.40</u>	0.41	0.41	<u>0.40</u>
160 hours					
MSE	28.84	22.11	24.28	24.16	<u>21.35</u>
MAE	4.13	3.63	3.78	3.77	<u>3.51</u>
RRSE	0.50	<u>0.44</u>	0.46	0.46	<u>0.44</u>

Table 3: **NY-TX Weather Results.**

AL Solar. We turn our focus to problems on the GNN end of the spatiotemporal spectrum where $N > L$. The AL Solar dataset is a middle ground that is still studied in the TSF literature (Lai et al. 2018) and consists of solar power production measurements taken at 10-minute intervals from 137 locations. We predict 4-hour sequences and the results are shown in Table 4. Our method is significantly more accurate than the TSF baselines. We speculate that this is due to an increased ability to forecast unusual changes in power production due to weather or other localized effects. `MTGNN` learns similar spatial relationships, but its temporal predictions are not as accurate.

	Linear AR	LSTNet	LSTM	MTGNN	Temporal	Spacetimeformer
MSE	14.3	15.09	14.35	11.40	14.3	<u>8.96</u>
MAE	2.29	2.08	2.02	1.76	1.85	<u>1.43</u>

Table 4: **AL Solar Results.**

Traffic Prediction. Next, we experiment on two datasets common in GNN research. The `Metr-LA` and `Pems-Bay` datasets consist of traffic speed readings at 5 minute intervals. We forecast the conditions for the next hour. In addition to the baselines in our research code, we include scores from the original `DCRNN` GNN model for context. Our method clearly separates itself from TSF models and enters the performance band of dedicated GNN methods - even those that rely on predefined road graphs.

	Time Series Models				GNN Models		
	Linear AR	LSTM	LSTNet	Temporal	DCRNN	MTGNN	Spacetimeformer
Metr-LA							
MAE	4.28	3.34	3.36	3.14	3.03	2.92	<u>2.82</u>
MSE	91.57	48.19	44.23	41.88	37.88	39	<u>36.21</u>
MAPE	11.11	9.89	9.53	8.9	8.27	8.46	<u>7.71</u>
Pems-Bay							
MAE	2.24	2.41	2.03	2.37	1.59	1.75	1.73
MSE	27.62	25.49	19.17	23.52	<u>12.81</u>	15.23	14.37
MAPE	4.98	5.81	4.68	5.52	<u>3.61</u>	4.08	3.85

Table 5: **Traffic Forecasting Results.**

Spatiotemporal Attention Patterns. Our method relies on approximate attention mechanisms that never explicitly compute the attention matrix. However, we use a trick described in the `Performer` appendix (Choromanski et al. 2021) to visualize attention patterns. Standard `Temporal Transformers` learn sliding patterns that resemble convolutions. These wave-like patterns are the result of `Time2Vec` information in the input. Our method learns distinct connections between variables - this leads to attention diagrams that tend to be structured in “variable blocks” due to the way we flatten our input sequence. Figure 4 provides an annotated example for the NY-TX weather dataset. If viewing a digital copy of this paper, the reader may be able to zoom in and see the wave-like temporal patterns that exist within each “block” of variable attention. Our method learns spatial attention over blocks of variable inputs and convolution-style temporal attention over the timesteps within each variable. Some attention heads convincingly recover the ground-truth relationship between input variables in the NY-TX weather dataset. GNN-level performance in highly spatial tasks like traffic forecasting supports a similar conclusion for more complex graphs.

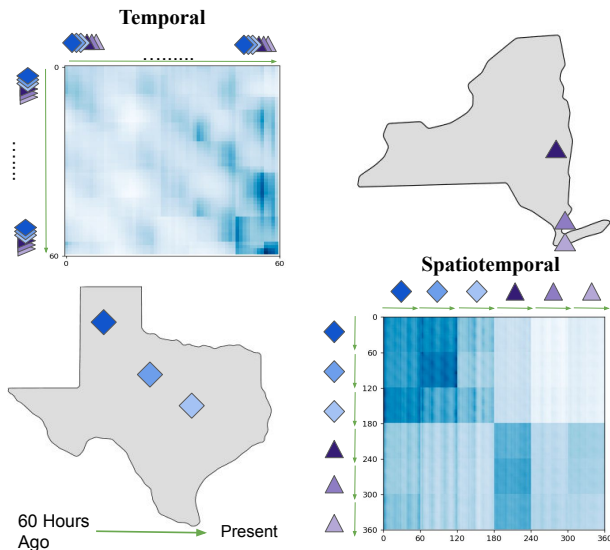


Figure 4: **Discovering Spatial Relationships from Data:** We forecast the temperature at three weather stations in Texas (lower left, blue) and three stations in New York (upper right, purple). Temporal attention models stack all six time series into one input variable and attend across time alone (upper left). By flattening the input and adding a spatial component to the existing time embedding, our method recovers the correct spatial relationship between the variables along with the strided temporal relation (lower right); nearby stations look to each other for relevant information about future weather patterns and ignore the stations hundreds of miles away. (Darker blue \rightarrow more attention).

Node Classification. During our development process, we became interested in the amount of spatial information that makes it through the encoder and decoder layers. We created a way to measure this by adding a softmax classification layer to the encoder and decoder output sequences. This layer interprets each token and outputs a prediction for the time series variable it originated from. Importantly, we detach this classification loss from the forecasting loss our model is optimizing; only the classification layer is trained on this objective. Classification accuracy begins near zero but spikes upwards of 99% in all problems within a few hundred gradient updates due to distinct (randomly initialized) variable embeddings that are well-preserved by the residual Pre-Norm Transformer architecture. In TSF tasks like NY-TX weather, this accuracy is maintained throughout training. However, in more spatial tasks like Metr-LA, accuracy begins to decline over time. Because this decline corresponds to increased forecasting accuracy, we interpret this as a positive indication that related nodes are grouped with similar variable embeddings that become difficult for a single-layer classification model to distinguish.

Ablations. Finally, we perform an ablation experiment on the NY-TX Weather and Metr-LA Traffic datasets. The results are shown in Table 6. The relative importance of space and time embedding information changes based on whether the problem is more temporal like NY-TX Weather or spatial like traffic forecasting. Metr-LA is the dataset that motivated

our use of Local Attention modules, and they are essential to performance. However, the model still relies on spatial embeddings, as removing this information along with global attention leads to the most inaccurate forecasts.

	MAE	Classification Acc. (%)
NY-TX Weather ($L = 200, N = 6$)		
Full Spatiotemporal	<u>2.57</u>	<u>99</u>
No Local Attention	2.62	<u>99</u>
No Space Embedding	2.66	45
Temporal Embedding	2.67	-
No Value Embedding	3.83	<u>99</u>
No Time Embedding	4.01	<u>99</u>
Metr-LA Traffic ($L = 24, N = 207$)		
Full Spatiotemporal	<u>2.82</u>	49
No Global Attention	2.87	35
No Time Embedding	3.11	50
Temporal Embedding	3.14	-
No Local Attention	3.27	<u>54</u>
No Space Embedding	3.29	2
No Global Attention, No Space Emb.	3.48	1

Table 6: **Ablation Results.**

5 Conclusion and Future Directions

This paper has presented a unified method for multivariate forecasting based on the application of Long-Range Transformer architectures to elongated spatiotemporal input sequences. Our approach jointly learns temporal and spatial relationships to achieve competitive results on long-sequence time series forecasting, and can scale to high dimensional spatial problems without relying on a predefined graph. We see at least two promising directions for future development. First, Long-Range Transformers are an active area of research; smaller memory footprints and increased computational resources are likely to improve performance and open up applications of this method to larger problems. Second, it is not clear that we are fully utilizing the dynamic graph capabilities of our method. Our model learns variable graphs across time and space jointly without assuming a fixed spatial relationship. However, GNN methods that do make this assumption have similar forecasting accuracy. It may be that adapting the relationship between variables over time has limited benefit in the benchmark datasets discussed. For example, traffic datasets contain some situations where adaptive graphs are beneficial (e.g. when intersection relationships change due to accidents or other road closures), however there are probably applications where this kind of temporal graph adjustment is more essential. The proposed method and future improvements may be more beneficial in these domains.

References

Araabi, A.; and Monz, C. 2020. Optimizing Transformer for Low-Resource Neural Machine Translation. arXiv:2011.02266.

- Arnab, A.; Deghani, M.; Heigold, G.; Sun, C.; Lučić, M.; and Schmid, C. 2021. ViViT: A Video Vision Transformer. *arXiv:2103.15691*.
- Benidis, K.; Rangapuram, S. S.; Flunkert, V.; Wang, B.; Maddix, D.; Turkmen, C.; Gasthaus, J.; Bohlke-Schneider, M.; Salinas, D.; Stella, L.; et al. 2020. Neural forecasting: Introduction and literature overview. *arXiv preprint arXiv:2004.10240*.
- Borovykh, A.; Bohte, S.; and Oosterlee, C. W. 2017. Conditional time series forecasting with convolutional neural networks. *arXiv preprint arXiv:1703.04691*.
- Box, G. E.; Jenkins, G. M.; Reinsel, G. C.; and Ljung, G. M. 2015. *Time series analysis: forecasting and control*. John Wiley & Sons.
- Bruna, J.; Zaremba, W.; Szlam, A.; and LeCun, Y. 2014. Spectral Networks and Locally Connected Networks on Graphs. *arXiv:1312.6203*.
- Cai, L.; Janowicz, K.; Mai, G.; Yan, B.; and Zhu, R. 2020. Traffic transformer: Capturing the continuity and periodicity of time series for traffic forecasting. *Transactions in GIS*, 24(3): 736–755.
- Cerqueira, V.; Torgo, L.; and Mozetič, I. 2020. Evaluating time series forecasting models: An empirical study on performance estimation methods. *Machine Learning*, 109(11): 1997–2028.
- Child, R.; Gray, S.; Radford, A.; and Sutskever, I. 2019. Generating long sequences with sparse transformers. *arXiv preprint arXiv:1904.10509*.
- Choromanski, K.; Likhoshesterov, V.; Dohan, D.; Song, X.; Gane, A.; Sarlos, T.; Hawkins, P.; Davis, J.; Mohiuddin, A.; Kaiser, L.; Belanger, D.; Colwell, L.; and Weller, A. 2021. Rethinking Attention with Performers. *arXiv:2009.14794*.
- Dettmers, T. 2020. Data Dropout for Wikitext-2 (Tweet #1247998807494684672).
- Devlin, J.; Chang, M.-W.; Lee, K.; and Toutanova, K. 2019. BERT: Pre-training of Deep Bidirectional Transformers for Language Understanding. *arXiv:1810.04805*.
- Falcon, e. a., WA. 2019. PyTorch Lightning. *GitHub. Note: <https://github.com/PyTorchLightning/pytorch-lightning>*, 3.
- Fan, A.; Grave, E.; and Joulin, A. 2019. Reducing Transformer Depth on Demand with Structured Dropout. *arXiv:1909.11556*.
- Gangopadhyay, T.; Tan, S. Y.; Jiang, Z.; Meng, R.; and Sarkar, S. 2021. Spatiotemporal attention for multivariate time series prediction and interpretation. In *ICASSP 2021-2021 IEEE International Conference on Acoustics, Speech and Signal Processing (ICASSP)*, 3560–3564. IEEE.
- Guo, Q.; Qiu, X.; Liu, P.; Shao, Y.; Xue, X.; and Zhang, Z. 2019. Star-transformer. *arXiv preprint arXiv:1902.09113*.
- Huang, X. S.; Perez, F.; Ba, J.; and Volkovs, M. 2020. Improving Transformer Optimization Through Better Initialization. In III, H. D.; and Singh, A., eds., *Proceedings of the 37th International Conference on Machine Learning*, volume 119 of *Proceedings of Machine Learning Research*, 4475–4483. PMLR.
- Iwata, T.; and Kumagai, A. 2020. Few-shot Learning for Time-series Forecasting. *arXiv preprint arXiv:2009.14379*.
- Joshi, C. 2020. Transformers are Graph Neural Networks. *The Gradient*.
- Kazemi, S. M.; Goel, R.; Eghbali, S.; Ramanan, J.; Sahota, J.; Thakur, S.; Wu, S.; Smyth, C.; Poupart, P.; and Brubaker, M. 2019. Time2vec: Learning a vector representation of time. *arXiv preprint arXiv:1907.05321*.
- Lai, G.; Chang, W.-C.; Yang, Y.; and Liu, H. 2018. Modeling Long- and Short-Term Temporal Patterns with Deep Neural Networks. *arXiv:1703.07015*.
- Lanchantin, J.; Weingarten, T.; Sekhon, A.; Miller, C.; and Qi, Y. 2021. Transfer Learning for Predicting Virus-Host Protein Interactions for Novel Virus Sequences. *bioRxiv*.
- Li, S.; Jin, X.; Xuan, Y.; Zhou, X.; Chen, W.; Wang, Y.-X.; and Yan, X. 2019. Enhancing the locality and breaking the memory bottleneck of transformer on time series forecasting. *Advances in Neural Information Processing Systems*, 32: 5243–5253.
- Li, Y.; Yu, R.; Shahabi, C.; and Liu, Y. 2018. Diffusion Convolutional Recurrent Neural Network: Data-Driven Traffic Forecasting. *arXiv:1707.01926*.
- Lim, B.; and Zohren, S. 2021. Time-series forecasting with deep learning: a survey. *Philosophical Transactions of the Royal Society A*, 379(2194): 20200209.
- Liu, L.; Liu, X.; Gao, J.; Chen, W.; and Han, J. 2020. Understanding the Difficulty of Training Transformers. *arXiv:2004.08249*.
- Liu, P.; Chang, S.; Huang, X.; Tang, J.; and Cheung, J. C. K. 2019. Contextualized non-local neural networks for sequence learning. In *Proceedings of the AAAI Conference on Artificial Intelligence*, volume 33, 6762–6769.
- Manakul, P.; and Gales, M. J. F. 2021. Long-Span Summarization via Local Attention and Content Selection. *arXiv:2105.03801*.
- Nguyen, T. Q.; and Salazar, J. 2019. Transformers without tears: Improving the normalization of self-attention. *arXiv preprint arXiv:1910.05895*.
- Oreshkin, B. N.; Carpov, D.; Chapados, N.; and Bengio, Y. 2020. Meta-learning framework with applications to zero-shot time-series forecasting. *arXiv:2002.02887*.
- Pappagari, R.; Żelasko, P.; Villalba, J.; Carmiel, Y.; and Dehak, N. 2019. Hierarchical Transformers for Long Document Classification. *arXiv:1910.10781*.
- Park, C.; Lee, C.; Bahng, H.; Tae, Y.; Jin, S.; Kim, K.; Ko, S.; and Choo, J. 2020. ST-GRAT: A Novel Spatio-temporal Graph Attention Networks for Accurately Forecasting Dynamically Changing Road Speed. *Proceedings of the 29th ACM International Conference on Information & Knowledge Management*.
- Paszke, A.; Gross, S.; Massa, F.; Lerer, A.; Bradbury, J.; Chanan, G.; Killeen, T.; Lin, Z.; Gimelshein, N.; Antiga, L.; Desmaison, A.; Kopf, A.; Yang, E.; DeVito, Z.; Raison, M.; Tejani, A.; Chilamkurthy, S.; Steiner, B.; Fang, L.; Bai, J.; and Chintala, S. 2019. PyTorch: An Imperative Style, High-Performance Deep Learning Library. In Wallach, H.;

- Larochelle, H.; Beygelzimer, A.; d'Alché-Buc, F.; Fox, E.; and Garnett, R., eds., *Advances in Neural Information Processing Systems 32*, 8024–8035. Curran Associates, Inc.
- Plizzari, C.; Cannici, M.; and Matteucci, M. 2021. Skeleton-based action recognition via spatial and temporal transformer networks. *Computer Vision and Image Understanding*, 208-209: 103219.
- Qin, Y.; Song, D.; Chen, H.; Cheng, W.; Jiang, G.; and Cottrell, G. 2017. A Dual-Stage Attention-Based Recurrent Neural Network for Time Series Prediction. arXiv:1704.02971.
- Salinas, D.; Flunkert, V.; and Gasthaus, J. 2019. DeepAR: Probabilistic Forecasting with Autoregressive Recurrent Networks. arXiv:1704.04110.
- Shen, S.; Yao, Z.; Gholami, A.; Mahoney, M. W.; and Keutzer, K. 2020. PowerNorm: Rethinking Batch Normalization in Transformers. arXiv:2003.07845.
- Shih, S.-Y.; Sun, F.-K.; and Lee, H.-y. 2019. Temporal pattern attention for multivariate time series forecasting. *Machine Learning*, 108(8): 1421–1441.
- Smyl, S. 2020. A hybrid method of exponential smoothing and recurrent neural networks for time series forecasting. *International Journal of Forecasting*, 36(1): 75–85.
- Tay, Y.; Dehghani, M.; Abnar, S.; Shen, Y.; Bahri, D.; Pham, P.; Rao, J.; Yang, L.; Ruder, S.; and Metzler, D. 2020. Long Range Arena: A Benchmark for Efficient Transformers. arXiv:2011.04006.
- Taylor, S. J.; and Letham, B. 2018. Forecasting at scale. *The American Statistician*, 72(1): 37–45.
- Vaswani, A.; Shazeer, N.; Parmar, N.; Uszkoreit, J.; Jones, L.; Gomez, A. N.; Kaiser, Ł.; and Polosukhin, I. 2017. Attention is all you need. In *Advances in neural information processing systems*, 5998–6008.
- Wang, S.; Li, B. Z.; Khabsa, M.; Fang, H.; and Ma, H. 2020. Linformer: Self-Attention with Linear Complexity. arXiv:2006.04768.
- Wu, S.; Xiao, X.; Ding, Q.; Zhao, P.; Ying, W.; and Huang, J. 2020a. Adversarial Sparse Transformer for Time Series Forecasting.
- Wu, Z.; Pan, S.; Chen, F.; Long, G.; Zhang, C.; and Yu, P. S. 2021a. A Comprehensive Survey on Graph Neural Networks. *IEEE Transactions on Neural Networks and Learning Systems*, 32(1): 4–24.
- Wu, Z.; Pan, S.; Long, G.; Jiang, J.; Chang, X.; and Zhang, C. 2020b. Connecting the Dots: Multivariate Time Series Forecasting with Graph Neural Networks. arXiv:2005.11650.
- Wu, Z.; Wu, L.; Meng, Q.; Xia, Y.; Xie, S.; Qin, T.; Dai, X.; and Liu, T.-Y. 2021b. UniDrop: A Simple yet Effective Technique to Improve Transformer without Extra Cost. arXiv:2104.04946.
- Xiong, R.; Yang, Y.; He, D.; Zheng, K.; Zheng, S.; Xing, C.; Zhang, H.; Lan, Y.; Wang, L.; and Liu, T.-Y. 2020. On Layer Normalization in the Transformer Architecture. arXiv:2002.04745.
- Xiong, Y.; Zeng, Z.; Chakraborty, R.; Tan, M.; Fung, G.; Li, Y.; and Singh, V. 2021. Nyströmformer: A Nyström-Based Algorithm for Approximating Self-Attention. arXiv:2102.03902.
- Xu, M.; Dai, W.; Liu, C.; Gao, X.; Lin, W.; Qi, G.-J.; and Xiong, H. 2021. Spatial-Temporal Transformer Networks for Traffic Flow Forecasting. arXiv:2001.02908.
- Ye, Z.; Guo, Q.; Gan, Q.; Qiu, X.; and Zhang, Z. 2019. Bp-transformer: Modelling long-range context via binary partitioning. *arXiv preprint arXiv:1911.04070*.
- Zaheer, M.; Guruganesh, G.; Dubey, K. A.; Ainslie, J.; Alberti, C.; Ontanon, S.; Pham, P.; Ravula, A.; Wang, Q.; Yang, L.; et al. 2020. Big Bird: Transformers for Longer Sequences. In *NeurIPS*.
- Zerveas, G.; Jayaraman, S.; Patel, D.; Bhamidipaty, A.; and Eickhoff, C. 2020. A Transformer-based Framework for Multivariate Time Series Representation Learning. *arXiv preprint arXiv:2010.02803*.
- Zhang, H.; Gong, Y.; Shen, Y.; Li, W.; Lv, J.; Duan, N.; and Chen, W. 2021. Poolingformer: Long Document Modeling with Pooling Attention. arXiv:2105.04371.
- Zhou, H.; Zhang, S.; Peng, J.; Zhang, S.; Li, J.; Xiong, H.; and Zhang, W. 2021. Informer: Beyond efficient transformer for long sequence time-series forecasting. In *Proceedings of AAAI*.
- Zhou, W.; Ge, T.; Xu, K.; Wei, F.; and Zhou, M. 2020. Scheduled DropHead: A Regularization Method for Transformer Models. arXiv:2004.13342.
- Zhu, C.; Ping, W.; Xiao, C.; Shoyebi, M.; Goldstein, T.; Anandkumar, A.; and Catanzaro, B. 2021. Long-Short Transformer: Efficient Transformers for Language and Vision. arXiv:2107.02192.

A Additional Related Work in Spatial/Temporal Transformers

As mentioned in Sec 2.3, there are several Transformer-based methods that include spatial attention layers. Despite heavy overlap in technical jargon (“spatial attention”, “temporal attention”), these are not TSF methods like our model but are instead GNN-style models that use MSA as a temporal learning mechanism. STTN (Xu et al. 2021), Traffic Transformer (Cai et al. 2020), ST-GRAT (Park et al. 2020), and ST-TR (Plizzari, Cannici, and Matteucci 2021) all rely on predefined adjacency matrices that represent the spatial connection between input variables. In most cases this is used in a fixed Graph Convolutional Layer, though STTN also uses the provided graph to initialize spatial and positional embeddings. In contrast, we learn the spatial relationships between variables during training and initialize embeddings randomly based on their index order. Most methods do not utilize a global concept of time; Traffic Transformer is an exception that primarily compares various time embeddings but does not consider Time2Vec and instead uses feed-forward projections of hand-engineered time features. All of these works focus on a specific domain (namely traffic forecasting with the exception of ST-TR’s skeleton classification). This paper experiments on problems ranging from traffic forecasting to more traditional long-sequence time series problems. These methods also divide spatial and temporal attention into separate learning subroutines - likely because this is both the norm in recent GNN literature and because hyper-efficient attention mechanisms capable of scaling to our superlong spatiotemporal sequences are a recent innovation. Combining spatial and temporal learning into a single attention mechanism is a simpler solution and may add the benefit of allowing earlier attention between distant temporal tokens. The one-shot approach explicitly allows for spatial relationships that change dynamically over time; some of these works are motivated by this goal but are forced to rely on their positional embeddings to achieve it (which do not include global time information). Finally, architectures like STTN do not contain target sequence self attention or cross attention with the encoded context sequence. They generate the entire sequence of target predictions with convolutional output layers. This makes it more difficult to stay consistent across long-term predictions, which is supported by our MTGNN baselines that use a similar output mechanism.

Although they are related works, we do not compare against these methods due to the requirement of a predefined graph that is not available in all experiments. Even in cases where ground-truth graphs are readily available, we find it more interesting to see if these relationships can be learned from scratch and still match state-of-the-art performance. To be fair, our method has no clear way of utilizing these graphs when they do exist, which could be considered a shortcoming in data-limited contexts.

B Dataset Details

- **Toy Dataset (based on (Shih, Sun, and Lee 2019)).** We generate D sequences where sequence i at timestep t is defined by:

$$Y_t^i = \sin\left(\frac{2\pi it}{64}\right) + \frac{1}{D+1} \sum_{j=1, j \neq i}^D \sin\left(\frac{2\pi jt}{64}\right) \quad (2)$$

We map 2,000 timesteps to a sequence of daily calendar dates beginning on Jan 1, 2000. We set $D = 20$ and use a context length of 128 and a target length of 32. Example curves are plotted in Figure 5.

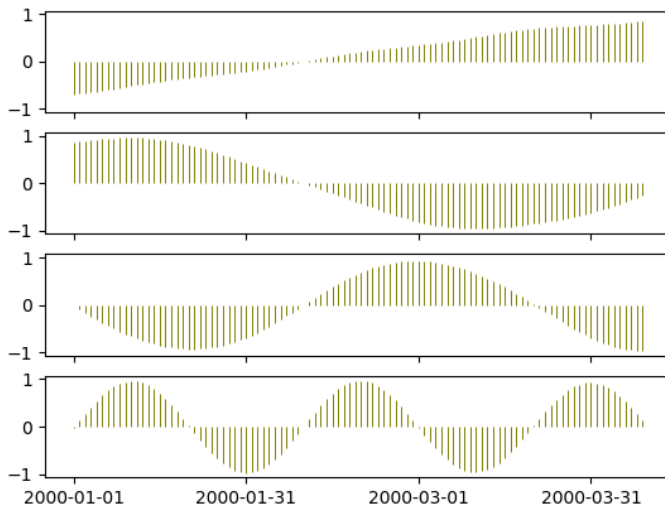


Figure 5: Toy Dataset Example.

- **NY-TX Weather (*new*)**. We obtain hourly temperature readings from the ASOS weather network. As described in our introductory example, we use three stations located in central Texas and three more located hundreds of miles away in eastern New York. The data covers the years 1949 – 2021, making this a very large dataset by TSF standards. Many of the longest active stations are airport weather stations. We use the airport codes ACT (Waco, TX), ABI (Abilene, TX), AMA (Amarillo, TX), ALB (Albany, New York) as well as the two largest airports in the New York City metro, LGA and JFK.
- **Metr-LA Traffic (Li et al. 2018)**. A popular benchmark dataset in the GNN literature consisting of traffic measurements from Los Angeles highway sensors at 6-minute intervals over 4 months in 2012. Both the context and target sequence lengths are set to 12. We use the same train/test splits as (Li et al. 2018).
- **AL Solar (Lai et al. 2018)**. A popular benchmark dataset in the time series literature consisting of solar power production measurements across the state of Alabama in 2006. We use a context length of 168 and a target length of 24.
- **Pems-Bay Traffic (Li et al. 2018)**. Similar to Metr-LA but covering the Bay Area over 6 months in 2017. The context and target lengths are 12 and we use the standard train/test split.

Normalization and Time Representation. We normalize the values of each variable sequence independently based on training set statistics. We represent calendar dates by splitting the information into separate year, month, day, hour, minute, and second values and then re-scaling each to be $\in [0, 1]$. This works out so that only the year value is unbounded; we divide by the latest year present in the training set. The reformatted calendar values form the input to the `Time2Vec` embedding layer. As a brief aside, the time embedding mechanism of our model could be used in situations where the context and target sequence timestamps are different for each variable (e.g., they are sampled at different intervals). We do not take advantage of this in our experimental results because it is not relevant to common benchmark datasets and is not applicable to all the baselines we consider.

C Model Details and Hyperparameters

C.1 Spacetimeformer Details

There is significant empirical work investigating technical improvements to the Transformer architecture and training routine (Huang et al. 2020) (Liu et al. 2020) (Xiong et al. 2020) (Nguyen and Salazar 2019) (Wu et al. 2021b) (Zhou et al. 2020) (Araabi and Monz 2020) (Fan, Grave, and Joulin 2019) (Shen et al. 2020). We incorporate some of these techniques to increase performance and hyperparameter robustness while retaining simplicity. A Pre-Norm architecture (Xiong et al. 2020) is used to forego the standard learning rate warmup phase. We also find that replacing `LayerNorm` with `BatchNorm` is advantageous in the timeseries domain. (Shen et al. 2020) argue that `BatchNorm` is more popular in Computer Vision applications because reduced training variance improves performance over the `LayerNorms` that are the default in NLP. Our experiments add empirical evidence that this may also be the case in timeseries problems. We also experiment with `PowerNorm` (Shen et al. 2020) and `ScaleNorm` (Nguyen and Salazar 2019) layers with mixed results. All four variants are included as a configurable hyperparameter in our open-source release.

As mentioned in Sec 3.2, the output of our model is a sequence of parameterized Normal distributions that folds the flattened spatiotemporal sequence back into its original concatenated format and discards predictions on start tokens. This lets us choose from several different loss functions. Most datasets use either Mean Squared Error (MSE) or Mean Absolute Error (MAE) based solely on the mean of the output distribution; in these cases the standard deviation outputs are untrained and should be ignored. We occasionally compare Root Relative Squared Error (RRSE) and Mean Absolute Percentage Error (MAPE) - though they are never used as an objective function. We also consider a Negative Log Likelihood (NLL) loss that maximizes the probability of the target sequence according to the output distribution and makes use of the model’s uncertainty estimates. An example of the prediction distributions learned by the NLL loss is shown in Figure 6.

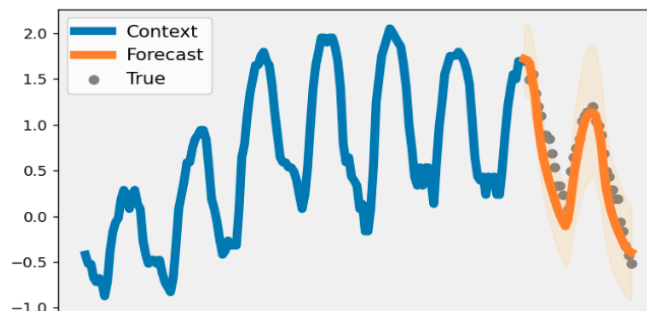


Figure 6: **Temperature Forecasts with Uncertainty.** Spatiotemporal Transformers with NLL loss functions increase prediction uncertainty along the target sequence and at daily low and high temperatures in the NY-TX Weather dataset.

TSF datasets are generally much smaller than their NLP counterparts. As a result, we employ a number of regularization techniques and tend to prefer narrower architectures than are common in NLP. We add dropout to the embedding layer,

query/key/value layers, feed-forward layers and attention outputs. Inspired by discussion on Transformer training on small NLP datasets (Dettmers 2020), we also experiment with full token dropout in which entire input tokens are zeroed after the embedding phase - with little success.

Our architecture consists of four types of attention (Fig 3). “Global Self Attention” and “Global Cross Attention” attend to the entire spatiotemporal sequence, while “Local Self Attention” and “Local Cross Attention” attend to the timesteps of a single variable in isolation. Many Long-Range Transformer architectures include a concept of “local” vs “global” attention. For example, BigBird (Zaheer et al. 2020), Star-Transformer (Guo et al. 2019) and BP-Transformer (Ye et al. 2019) connect each token to local tokens in addition to global tokens. In these methods, “local” tokens are *adjacent* in terms of sequence order. This aligns well with the assumption that NLP sequences have meaningful order. Our flattened spatiotemporal sequence complicates that assumption because tokens can be adjacent while originating from different variables at vastly different timesteps. Regardless, we use the term “local” in a spatial sense where it refers to all timesteps within a single variable. Our local attention is straightforwardly implemented on top of any open-source MSA variant by splitting the spatiotemporal sequence into its separate variables, folding this extra dimension into the batch dimension, performing attention as normal and then reversing the transformation. The attention mechanism used in all four types is configurable, and our open-source release includes ProbSparse Self Attention (Zhou et al. 2021), Nystromformer Self Attention (Xiong et al. 2021), Performer Self/Cross Attention in addition to the standard Self/Cross Full Attention. In practice, the sequence lengths considered in this paper require Performer Global Attention. The Local Attention modules are much more flexible; we default to Performer for simplicity.

Table 7 provides an overview of the hyperparameters used in our experiments. The values were determined by a brief sweep based on validation loss. It is worth reiterating that these models are quite small relative to Informer and tiny in comparison to standard NLP architectures (Vaswani et al. 2017). The architectures listed in Table 7 consist of 1 – 3M parameters. The memory requirements of our model are a central engineering challenge in this work, but Transformers do scale well with sequence length in terms of total parameter count. In contrast, methods like MTGNN grow larger with L and can become significantly larger than our model in datasets like NY-TX Weather or AL Solar. Temporal-only ablations add an extra encoder and decoder layer to help even out the difference in parameter count that comes with skipping local attention modules.

	NY-TX Weather	AL Solar	Metr-LA	Pems-Bay	Toy
<i>Model Dim</i>	200	128	128	128	100
<i>FF Dim</i>	800	512	512	512	400
<i>Attn Heads</i>	8	8	8	8	4
<i>Enc Layers</i>	2	3	5	4	4
<i>Dec Layers</i>	2	3	4	4	4
<i>Initial Convs</i>	0	1	0	0	0
<i>Inter. Convs</i>	0	0	0	0	0
<i>Local Self Attn</i>	performer	performer	performer	performer	performer
<i>Local Cross Attn</i>	performer	performer	performer	performer	performer
<i>Global Self Attn</i>	performer	performer	performer	performer	performer
<i>Global Cross Attn</i>	performer	performer	performer	performer	performer
<i>Normalization</i>	batch	batch	batch	batch	batch
<i>Start Token Len</i>	(8, 16, 32)	8	3	3	4
<i>Time Emb Dim</i>	12	12	12	12	12
<i>Dropout FF</i>	0.2	0.3	0.3	0.4	.3
<i>Dropout Q/K/V</i>	0	0	0	0	0
<i>Dropout Token</i>	0	0	0	0	0
<i>Dropout Emb</i>	0.1	0.2	0.3	0.3	0
<i>L2 Weight</i>	0.01	0.01	0.01	0.01	0

Table 7: **Hyperparameters for Spacetimeformer main experiments.**

C.2 Baseline Details

In addition to variants/ablations of our Transformer framework, we consider several other Deep Learning architectures for TSF:

- **Linear AR:** A simple autoregressive linear model that acts independently on each input variable.
- **LSTNet (Lai et al. 2018):** A mix of RNN and Conv1D layers with skip connections that predicts the difference between the final output and the above linear model. The fully autoregressive approach does not scale well with some of the sequence lengths considered in this paper. For this reason, we do not use LSTNet in all experiments.

- **LSTM:** A standard encoder-decoder RNN without attention. We use scheduled sampling to anneal the teacher forcing training mechanism.
- **MTGNN (Wu et al. 2020b):** A GNN model that learns the adjacency matrix between its input variables. MTGNN one-shots the entire prediction sequence like our Transformer models. We use the annealed time mask that acts as a curriculum to emphasize shorter predictions early in training.

We use published hyperparameters on datasets that appear in the original work, and perform a sweep when they do not. Tricks like the linear delta in LSTNet and time mask curriculum in MTGNN are implemented for all models in our public code release; for simplicity’s sake we do not use them in the Transformer results. The evaluation statistics listed in all main tables are the average of three random seeds. We do not include variance measurements for readability. However, all the methods are quite consistent and the variance of the main Transformer models studied is essentially negligible.

`Time2Vec` is a key component of our embedding pipeline; the `Time2Vec` paper (Kazemi et al. 2019) finds that learned time representations improve many types of sequence models. We account for this potential advantage by applying `Time2Vec` to LSTM and MTGNN models with the same embedding dimension used in the Spacetimeformer embedding scheme. Linear AR and LSTNet do not have a clear way to include them but are less competitive in general.

C.3 Training and Evaluation Process

All models use the same basic training loop for a fair comparison. We use Early Stopping with a patience of 5 epochs and reduce learning rates on validation loss plateaus. Most datasets are evaluated at the end of each full epoch; NY-TX Weather is so large that we adjust this to every quarter epoch. As a final training detail, some datasets contain missing values that should be ignored during training. Of the datasets officially listed in this paper this only applies to Metr-LA and Pems-Bay. We adopt the “masked” loss functions used in DCRNN (Li et al. 2018): targets and predictions corresponding to missing timesteps are zeroed so that they do not impact gradient computation. Ignoring this detail is unfortunately a common bug in the literature and leads to falsely inaccurate results that are commonly reprinted in related work despite later corrections to the DCRNN results. Our traffic forecasting results (Table 5) use scores directly from updated log files rather than the original paper.

C.4 Code Implementation and Acknowledgements

The code for our method as well as the baselines and datasets can be found here ([github](#)). All models are implemented in PyTorch (Paszke et al. 2019) and the training process is conducted with PyTorch Lightning (Falcon 2019). Our LSTNet and MTGNN implementations are based on public code and verified by replicating experiments from the original papers. Generic models like LSTM and Linear AR are implemented from scratch and we made an effort to ensure the results are competitive. The code for the Spacetimeformer model was originally based on the Informer open-source release. Their code was a very helpful starting point although the many engineering changes associated with our work have led to significant changes.